



Open Access : : ISSN 1847-9286

[www.jESE-online.org](http://www.jESE-online.org)*Original scientific paper*

## Ellipsometric study of passive and anodic oxide films formed on Ti and Nb electrodes

Ljubomir Arsov<sup>✉</sup>, Irena Mickova*Faculty of Technology and Metallurgy, University Ss. Cyril and Methodius, Rudjer Boskovic 16, 1000 Skopje, Republic of Macedonia*<sup>✉</sup>Corresponding Author: [arsov@tmf.ukim.edu.mk](mailto:arsov@tmf.ukim.edu.mk); Tel. +389 2 3088 43; Fax: + 389 2 3 065 389

Received: October 20, 2015; Accepted: November 26, 2015

---

### Abstract

*Electrochemical formation of passive films and active/passive transition on Ti and Nb metal surfaces in various concentrations of H<sub>2</sub>SO<sub>4</sub> and KOH solutions was investigated using potentiostatic and cyclic voltammetry methods. By simultaneous electrochemical and in-situ ellipsometric measurements the coefficients of film thickness growth of passive films in the potential region from -1.5 V to 4 V were determined. Results indicate the strong influence of the concentration and electrolyte nature to the active/passive transitions and stability of passive films. The influence of cathodic pre-treatment on the passive films dissolution and appearance of the reactivation peaks during the reverse potential cycling were shown. By multiple cycle sequences in which the final anodic potential was gradually enlarged, the barrier properties of passive films on investigated electrodes were confirmed. The electrochemical and ellipsometric data showed that the passive films formed on Nb electrode are more resistant than passive films formed on Ti electrode, especially in higher concentrations of investigated aggressive solutions.*

### Keywords

Potentiostatic method, Cyclic voltammetry, Film thickness growth, Stability and reactivation of passive films

---

### Introduction

Over the past 50 years there has been a growing interest for the use of titanium and niobium, as well as their alloys, in various branches of the chemical and mechanical industry as construction materials, specifically in transport and stocking of aggressive fluids. They have been also used in electro-synthesis, solar energy conversion bio-medical and air-space applications. Research on the electrochemical behavior of Ti and Nb have covered the wide range of topics as

active-passive transition [1-2], formation of anodic oxide films [3-4], structure and chemical composition, breakdown processes [5-6], semi-conducting and optical properties [7-8] etc. Titanium and niobium belong to the group of valve metals because they develop spontaneously the stable passivating layers either when contacting air and/or water solutions. These layers in reality are natural oxide films, which are always present on Ti and Nb surfaces and explain their high corrosion resistance. In order to increase the corrosion resistance of Ti and Nb, the natural oxide films can be controllably thickened by anodic oxidation in appropriate electrolytes or by thermal oxidation in atmospheric conditions [9,10]. The anodic oxide film formation on Ti and Nb electrodes have been studied in some acid and alkaline electrolytes, using ellipsometry and other electrochemical and optical techniques, but generally for potentials/voltages higher than the trans-passive region [11,12]. Although the studies of metal passivity exist for almost 200 years, in literature data can be found very rarely the use of ellipsometric methods for determining the film thickness only in passive region during the cyclic voltammetry CV measurements. A few information's can be found in ref. [13] about the formation of passive films on Ti electrode in 0.1 M  $\text{H}_2\text{SO}_4$  depending of sweep rate and in one of our recent papers concerning the thickness growth and dissolution of electrochemical passive film on Nb in 10 M KOH [14].

The purpose of present investigations is to study the active passive transition of Ti and Nb electrodes, simultaneously with in-situ ellipsometric measurements. In that way is expected to get valuable results about the film thickness growth for each applied potential during the potentiostatic and CV scans measurements in forward and reverse potential directions. The comparative studies of Ti and Nb in acidic and alkaline solutions are carried out.

## Experimental

**Electrodes.** Massive cylindrical Ti and Nb rods (Alfa Aesar, Johnson Matthey Company), with purity 99.95 % and 99.8 % respectively and with 12.7 mm dia., were cut in disc species with length of 10 mm which were served as the working electrodes. On one basis of the disc a stout cooper wire was employed as the electrical contact. The discs were fitted into glass tubing of appropriate internal diameters by an epoxy resin (Struers), leaving the other basis with surface area of 1.27  $\text{cm}^2$  to contact the solution. Before each experiment the electrode surfaces were mechanically polished using metallographic emery paper 600 and then electro-polished to the mirror brightness in the baths: (i) for Ti electrodes containing: 60 ml perchloric acid + 540 ml methyl alcohol + 350 ml ethylene glycol mono butyl ether. The electro polishing conditions are given in ref. [15], (ii) for Nb electrodes containing: 170 ml nitric acid + 50 ml. hydro fluoric acid + 510 ml methyl alcohol + 5 g citric acid at voltage of 15.2 V. After electro-polishing the electrodes were rinsed with re-distilled water, ultrasonically cleaned in ethanol and finally dried using argon gas under pressure.

The counter electrode was a Pt grid with large surface area. The reference electrode was a saturated calomel electrode (SCE) in acidic aqueous solutions and mercury oxide electrode in alkaline aqueous solution. The potentials in this work are presented against using reference electrode. To avoid contamination, the reference electrodes were connected to the working electrode through the bridges with a Luggin capillary filled with the test solutions. After each experiment the working electrodes were mechanically re-polished and prepared for the next measurements using the procedures of electro-polishing as described above.

**Optical Electrolytic cell.** A three compartment optical electrolytic cell with an inlet and outlet for bubbling inert gas was adopted for electrochemical and ellipsometric in-situ measurements. Experiments were done in a Pyrex vessel with two optical quartz widows fixed at an angle of  $70^\circ$ .

The specimen surfaces were mounted vertically, with a rigid clamping system having adjustments for rotation, tilt and central positioning in the cell. Details of the design of this optical electrolytic cell are given elsewhere [16]. Prior to each experiment, when the electrode was immersed in the electrolyte solution, the electrolyte in the cell was de-aerated by flowing argon gas through a fritted bubbler for at least 30 min. before the run. The gas flow was disconnected during the run.

**Solutions.** Aqueous solutions Merck p.a. with concentrations of 1 M H<sub>2</sub>SO<sub>4</sub>, 3 M H<sub>2</sub>SO<sub>4</sub>, 1 M KOH and 6 M KOH was prepared in re-distilled and de-ionized water. After each experiment the electrolyte in the cell was exchanged in order to avoid eventual build-up of soluble Ti or Nb species.

**Apparatus.** The electrochemical measurements were carried out potentiostatically and potentiodynamic using HEKA model 488 potentiostat/galvanostat connected to a personal computer.

The ellipsometric measurements were performed with a Rudolph Research type 43603-200 thin-film ellipsometer at a wavelength of 546.1 nm and an incident angle of 70°

## Results and discussion

Electrochemical passivity of Ti and Nb has been mainly studied using galvanostatic, potentiostatic, potentiodynamic and EIS techniques [17-20]. In this paper we used potentiostatic and potentiodynamic methods combined with ellipsometry. Ellipsometry, also known as reflection polarimetry, is a very precise method for determining the optical constants, thickness and nature of reflecting surface, especially the metal surfaces with and without existence the thin films on them. This method derives its name from the measurements of the elliptically polarized light results from optical reflection from the investigate surface [21]. Hence, ellipsometry finds applicability in a wide variety of fields such as physical, chemical and micro-electronic engineering, corrosion, electrochemical and chemical formation of passive layers on metals, oxides, polymer films semiconductors, biology, medicine etc. The main strength of this technique lies in its capability to allow in-situ measurements and simultaneous determination of many optical parameters necessary to quantify the investigated system. The new generation of ellipsometers allows determination the film thicknesses of from 0.1 nm to 30 μm.

In ellipsometric measurements the experimentally measured parameters  $\Delta$  and  $\psi$  are related to the physical properties of the system by the use of Fresnel's equation

$$\rho = r_p / r_s = \tan \psi \cdot \exp(i \cdot \Delta) \quad (1)$$

In Eq. 1,  $\tan \psi$  represents relative amplitude attenuation,  $\Delta$  is relative phase change,  $i$  is imaginary number,  $r_p$  and  $r_s$  represent the Fresnel reflection coefficients for electromagnetic wave polarized parallel and perpendicular to the plane of incidence, respectively. For a three component system, the ellipsometric parameters  $\Delta$  and  $\psi$  are complex function of the following parameters.

$$\tan \psi \cdot \exp(i \cdot \Delta) = (\hat{n}_m, \hat{n}_f, \hat{n}_s, d, \lambda, \phi) \quad (2)$$

In Eq. 2,  $\hat{n}_m$  is complex refractive index of medium,  $\hat{n}_f$  - complex index of film,  $\hat{n}_s$  - complex index of metal substrate,  $d$  - film thickness,  $\lambda$  - wavelength of incidence electromagnetic wave and  $\phi$  - angle of incidence. To minimize the unknown parameters in Fresnel's equation the refractive index of medium (electrolytic solutions) could be determine with Abbe's refractometer, refractive index of metal substrate by some separate methods, for example ellipsometrical measurements in

vacuum of evaporated metal on microscope glasses. The other parameters as: wavelength  $\lambda$ , was given in dependence of used laser and angle of incidence  $\phi$  was adjusted to the ellipsometer. By method of mathematical iteration, using computer program, the film thickness and complex index of refraction are determined. In our case the experimentally measured parameters  $\Delta$  and  $\psi$  are fitted with theoretically calculated curves for  $\Delta$  and  $\psi$  for increasing direction of film thickness for in advance given step of film growth.

#### *Passive film on titanium electrode*

After electropolishing, the Ti electrodes were immersed in  $\text{H}_2\text{SO}_4$  solutions with various concentrations and open circuit potential, OCP, was recorded during the establishment of steady state potential, *i.e.* when the variations of potentials with time are negligible. The potentiostatic measurements were initiated from steady state potential with successive increasing the potential on the same electrode up to begin the evolution of oxygen in trans-passive region. Then, on the same electrode the potential was also successively changed in the reverse, cathodic direction up to value of starting potential. The variation of currents with time during establishment of steady state conditions were recorded for each successive change of potential. The steady state currents were then taken in construction of potentiostatic curves. Fig. 1 (a) illustrates the profile of one typical potentiostatic curve in the potential region from 0.75 to 3.5 V. In the first forward scan an active dissolution region exists and the anodic current increases exponentially with potential up to point *a*, where the anodic current peak is formed. In this region two processes take place: metal dissolution and in the same time growth of anodic oxide film. However, the metal dissolution is prevalent process. In the second region the anodic current decreases toward a low value corresponding to the beginning of the passivation. The passive film formation and its growth with imposed potential are followed with long current plateau whose values are near to zero. The third region corresponds to trans-passive region, point *c*, where anodic current begin again to increase. In the first forward scan simultaneously with potentiostatic current-voltage, the ellipsometric measurements were also performed during imposed potentials. From ellipsometrically measured parameters  $\Delta$  and  $\psi$  the film thicknesses were calculated, presented in fig. 1 (b). For calculation the film thicknesses the input data in equation (1) and (2) were: for 3M  $\text{H}_2\text{SO}_4$   $\hat{n}_m = 1.364$ , for virgin Ti substrate  $\hat{n}_s = 2.94(1-1.217i)$ , for wavelength of incident light  $\lambda = 546.1$  nm and for angle of incidence  $\phi = 70^\circ$ , whereas the unknown values of  $\hat{n}_f$  and *d* were calculated by fitting the theoretical data to the experimentally measure ones. The fitting procedure was performed by a special prepared computer program in which  $\hat{n}_f$  was searched for prior given values of the thicknesses in increments' of 1 nm, in an increasing direction. The number of theoretical  $\Delta - \psi$  points on the theoretical fitted curves depend of the thickness increments' given from our side. Taking into account that our ellipsometric measurements were performed in one relatively short potential region where the final film thickness at the end of the passive region is relatively low, the large dispersion of experimental points from the theoretically fitted curves is expected. During the computation only one theoretical function  $T = f(\Delta T - \psi T)$  was searched from the family of theoretical functions which had minimal distance to the experimental measured points  $\Delta E - \psi E$ . In determination the thicknesses of passive films the theoretical values of  $(\Delta T - \psi T)$  were taken in consideration whereas experimental dispersion of measure points  $(\Delta E - \psi E)$  were neglected. Details of computer program and fitting procedure are given in ref. [22].

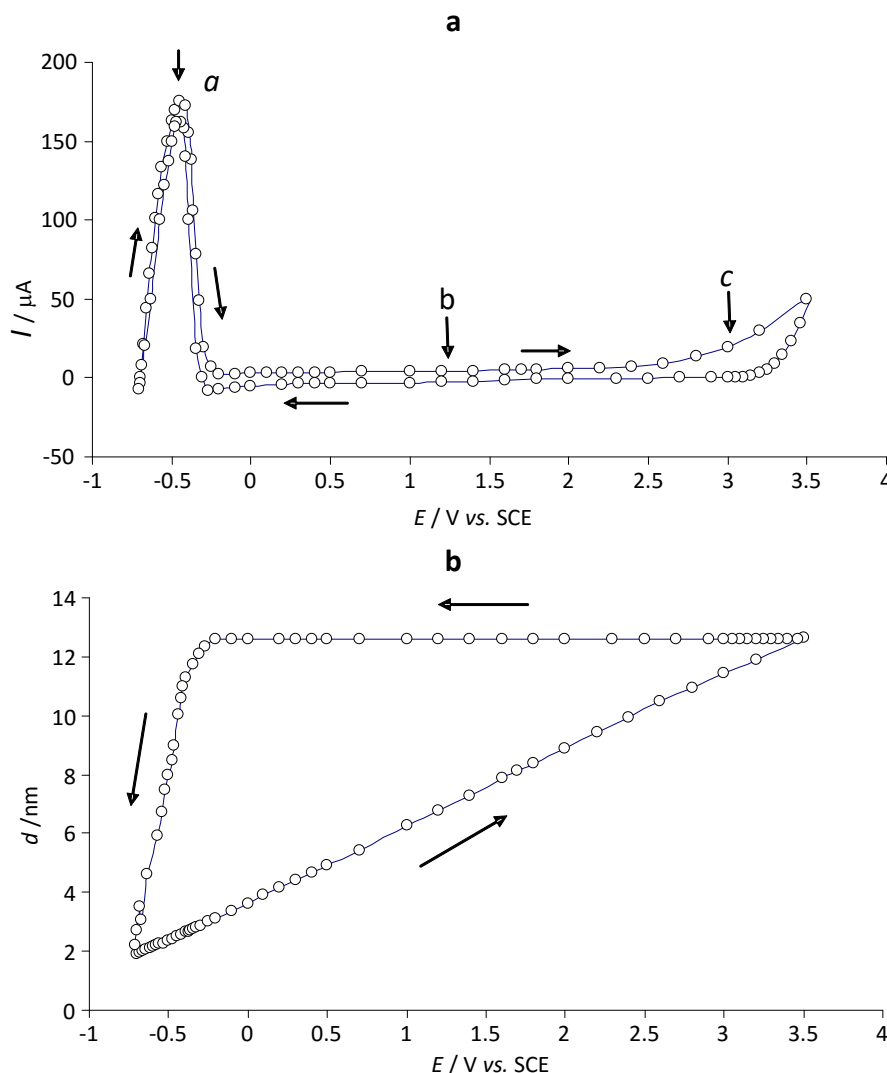


**Fig. 1.** (a) Potentiostatic  $I - E$  curve obtained on electropolished Ti surface in 3 M H<sub>2</sub>SO<sub>4</sub>,  
(b) Simultaneous determination the thickness of passive film by ellipsometry

As it can be seen from Fig. 1 (b) in the forward cycle the film thickness increases almost linearly and there is no noticeable dispersion of points which present growth of film thickness. From the slope of the forward curve the coefficient of film thickness growth is determined, i.e.  $\alpha = 2.51 \text{ nm/V}$ . In the reverse potential scan, with decrease of imposed potential in the cathodic direction up to a potential of -0.25 V, the long current plateau with current values also near to zero is observed. In this potential region ellipsometric measurements show that the thickness of the already formed passive film has a constant value and there is no indication for its dissolution and thinning. At a potential of -0.25 V the reactivation process begins with a sharp increase of anodic currents indicating electrochemical dissolution of the formed passive film. The reactivation peak already covers the activation. In the potential region between -0.25 V and -0.75 V, corresponding to the reactivation processes, the passive film was subject of continuous thinning and at the final potential of -0.75 V the film thickness is minimized and already has the same value as at the starting potential of the first forward scan. This indicates that the formed passive film is completely dissolved.

### Passive film on niobium electrode

In the similar way as in case of Ti, the Nb electrode was electropolished and then immersed in  $H_2SO_4$  solutions with various concentrations and the OCP was recorded during the establishment of steady state potential. The potentiodynamic measurements were initiated at potential of -0.75 V where a considerable cathodic current is observed and ended at 1 V (SCE), fig. 2(a)

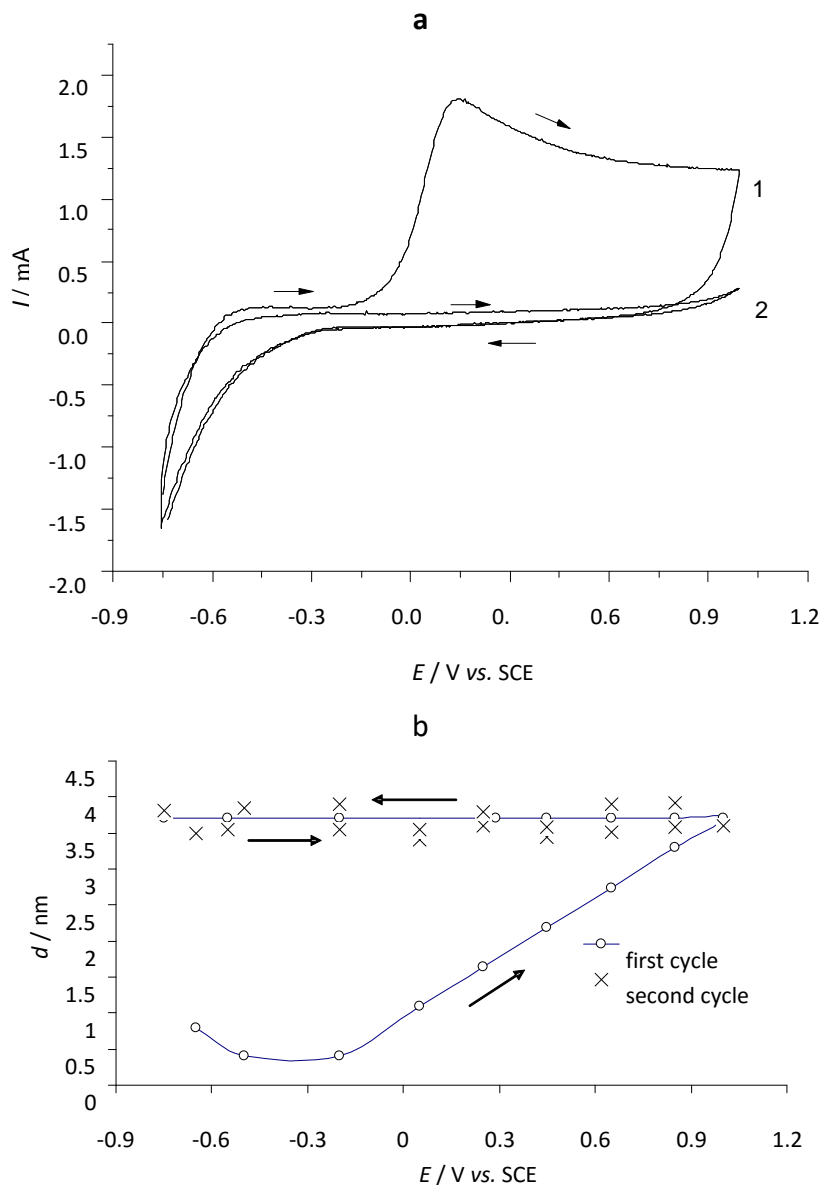


**Fig. 2.** (a) Voltammograms of Nb recorded in 10 M  $H_2SO_4$ , 1 – first cycle, 2 – second cycle;  
(b) Simultaneous determination the thickness of passive film by ellipsometry

In the first forward scan the cathodic current approaches zero value and when it get anodic values the process of metal dissolution and in the same time formation of anodic oxide films occur, as in case of titanium electrode. The active-passive transition exists in all investigated concentrations, but with increasing the concentration of  $H_2SO_4$  this process is more pronounced. During the reverse scan the reactivation processes or reduction of the already formed passive films were no recorded, even in high concentration of  $H_2SO_4$  up to 10 M. This was the main reason why our measurements started at more cathodic potential where the noticeable cathodic current appears in the beginning of the first forward scan and in each other next subsequent scans. It was expected that the natural or later formed passive films will be reduced at second scan during the

cathodic polarization of electrode. But the passive film formed in first forward scan cannot be cathodically reduced in the reverse scan. In the second cycle a constant current close to zero, for both, forward and reverse scans were recorded. The voltammograms in the next subsequent scans were almost identical to the second one. It is evident that after the first cycle, the Nb electrode remained passive over the whole investigated potential region and the formed passive film blocked all possible redox reaction at the Nb/passive film/electrolyte interface. Comparing the CV curves between Nb and Ti electrode it can be concluded that in  $\text{H}_2\text{SO}_4$  solution the Nb is corrosion more resistant than Ti electrode. During the CV scans simultaneous ellipsometric measurements were also performed, as in case of titanium electrode. From ellipsometric parameters  $\Delta$  and  $\Psi$  the film thicknesses were calculated (Fig. 2 (b)). In the beginning of the measurements, when cathodic current passes through the electrochemical cell, small decrease of the film thickness is observed, probably due to the partly dissolution of natural oxide film. With appearance of anodic current begins growth of anodic oxide film which is linear function up to the final anodic potential of 1 volt. From the slope of this linear curve the coefficient of film thickness growth of  $\alpha = 2.58 \text{ nm/V}$  was determined. In the first reverse scan the thicknesses of the film have constant values up to the starting potential of  $-0.75 \text{ V}$ . In the second and subsequent scans the thickness of the film has almost the same constant values, as in the end of first forward and reverse scan. The dispersion of the measured points in the second scans could be observed, probably for small dissolutions of the passive film and its reparation during the potential scan, or by existing of some side reactions.

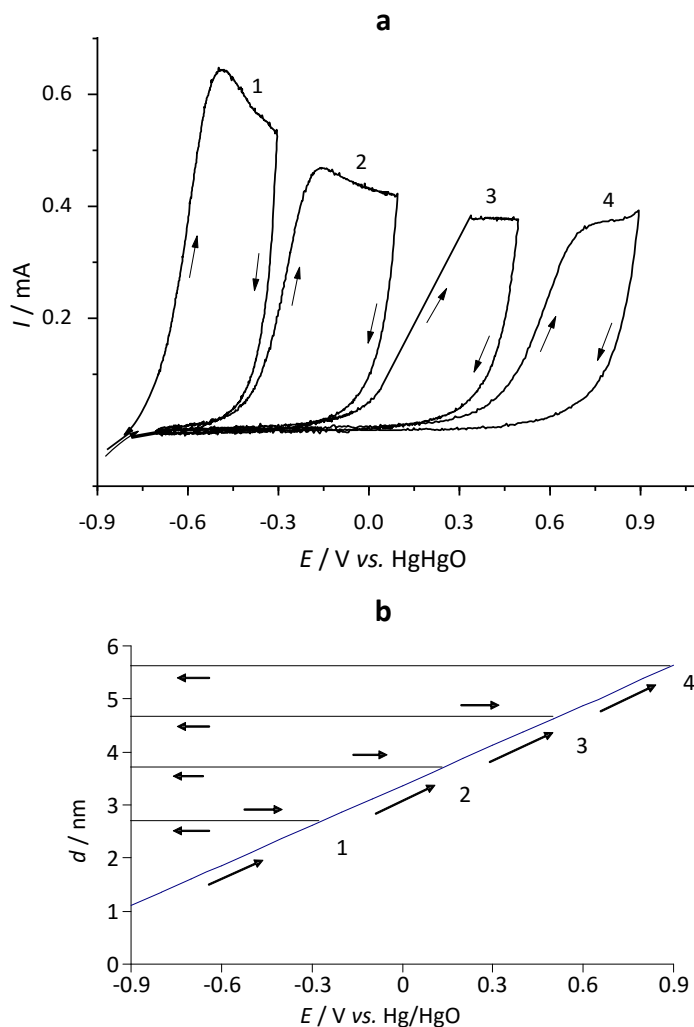


**Fig. 3.** (a) Multiple cycle sequences at increasing final anodic voltage of Nb recorded in 1M KOH; 1, 2, 3, and 4 represent number of cycle, (b) Simulated film thickness growth in each subsequent cycle



Fig. 3 (a) shows sequences of CV measurements where the final anodic potential on Nb in 1 M KOH is gradually enlarged in each next cycle. All subsequent presented voltammograms started from the same cathodic potential of -0.9 V and also finished to the same cathodic potential of -0.9 V. The difference in measurements is only to the increasing of final anodic potential. The progress of film thickness growth with anodic potential may take place only if the actual potential exceeds the maximum value attained in the previous cycle. The shapes of the sequences recorded in fig. 3 (a) represent just the copy segments of the corresponding voltammogram recorded from the starting potential at -0.9 V to final potential at 0.9 V at once, without sequences. The simulated film thickness growth that should be obtained by ellipsometric measurements are presented in fig.3 (b).

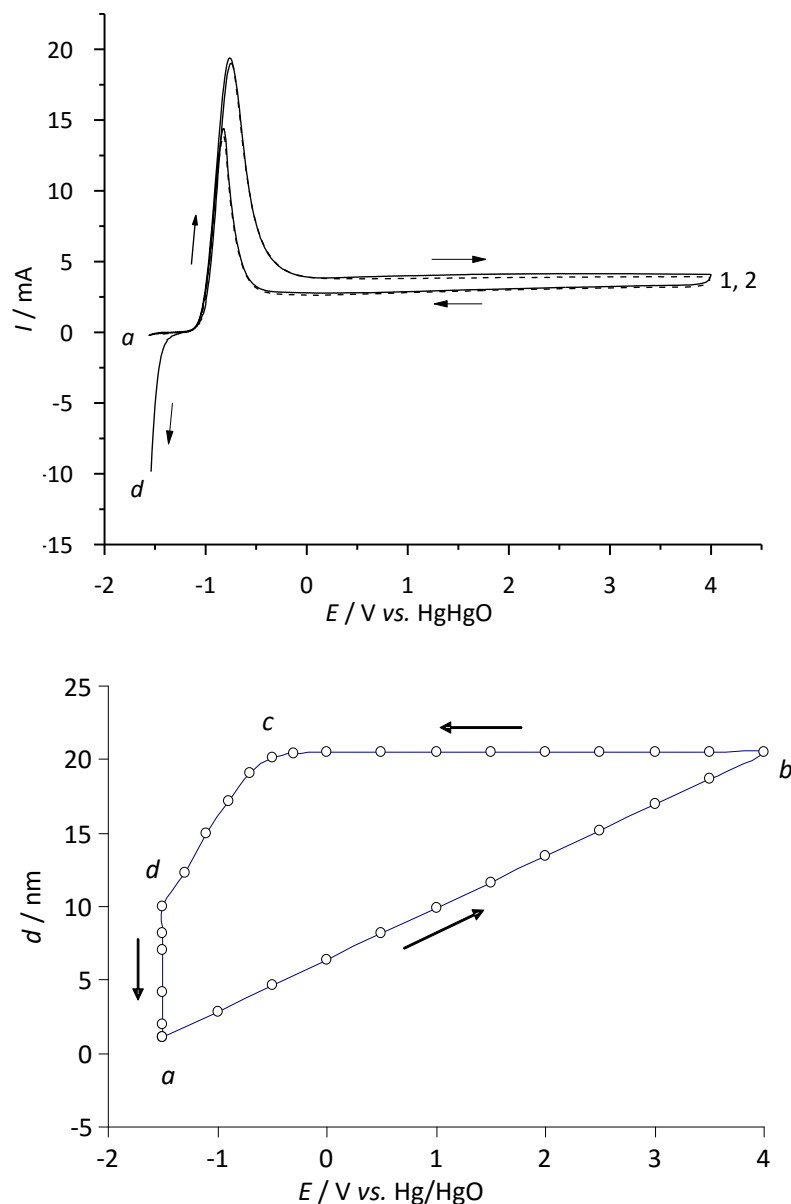


**Fig. 4.** (a) Voltammograms of Nb recorded in 6 M KOH, a – initial current at potential of -1.5 V, d – final current at potential of -1.5 V, 1 – first cycle, 2 – second cycle; (b) Simultaneous determination the thickness of passive film by ellipsometry, a – initial potential, b – final anodic potential, c – beginning of reactivation process, d – final potential at -1.5 V after the first cycle, d-a – cathodic dissolution at -1.5 V during 15 min of the rest film thickness after its partly dissolution in the reverse scan.



For each sequence, film thickness growth in the first forward scan and has constant value in the reverse scans. For each next sequence, in the first forward scan the film thickness has constant value up to the end of previous cycle and then continues to grow up to the final anodic potential. It is evident that by gradually increasing the final anodic potential the passive film grows by additional building of the new film on the already existing. The experiments in fig. 3, confirm the barrier properties of anodic oxide film build on the Nb surface.

The voltammograms recorded on Nb at the higher concentration of 6 M KOH are shown in Fig. 4 (a). The starting cathodic potential was at -1.5 V and final anodic potential at 4 V. In the first forward scan at the initial potential of -1.5 V, point *a*, a small cathodic current occurs and then in the anodic direction active/passive transition is recorded. In the reverse scan, at potential of about -0.5 V, begin reactivation process which partly covers the activation region. This suggested that with appearance of reactivation peak only part of the formed passive film is dissolved. At the end of the first reverse cycle, at cathodic potential of -1.5 V, point *d*, the noticeable cathodic current flows through the electrochemical cell. If we keep for example 15 min. the electrode at this potential and then initiate the second cycle, the voltammogram of the second cycle will be completely the same as in the first cycle. This indicates that after the first cycle, with keeping of some period of time the Nb electrode at -1.5 V, the previously formed passive film in the first cycle will be completely dissolved. The simultaneous ellipsometric measurements of the film thickness growth, presented in fig. 4 (b), showed continuous increasing of film thickness in the first forward scan and constant thickness values in the first reverse scan up to -0.5 V where begin reactivation process. In the region of reactivation peak the film thickness partly decrease and did not reaches the initial value at -1.5 V, as before starting the CV measurements. During the keeping the electrode at potential of -1.5 V, the film dissolution continue and finally it get the same value as in the beginning of the first forward scan.

## Conclusions

From potentiostatic and potentiodynamic measurements of Ti and Nb electrode in H<sub>2</sub>SO<sub>4</sub> and KOH solutions, simultaneous with ellipsometric in-situ measurements, the following conclusions can be drawn: (i) Comparative studies of mechanically polished and electropolished metal surfaces have shown that the dispersion of experimental points from the theoretically fitted curves is smaller for electropolished metal surfaces. It should be noted that during the fine mechanical polishing with diamond spray, smooth surfaces with mirror brightness were obtained. However, mechanical polishing leaves numerous micro-surface scratches and defects with random distributions which cause areas of differing electrical potentials due to surface stress. This is the main reason why in this work we used electropolished metal surfaces instead of fine mechanical polished. (ii) The potentiostatic and potentiodynamic curves of Ti and Nb recorded in all investigation concentrations of H<sub>2</sub>SO<sub>4</sub> and KOH solutions showed active passive transition with formation of passive films which are stable in lower concentration of investigated solution. (iii) For all investigated concentration of H<sub>2</sub>SO<sub>4</sub> and KOH solutions, the passive film thickness growth on Ti and Nb electrodes are linear function with applied potential, up to final anodic potential in the forward scan. (iv) For Ti electrode in 3M H<sub>2</sub>SO<sub>4</sub>, the passive films formed in the forward potentials were completely dissolved in the reverse potentials, where reactivation process was recorded. (v) For Nb, even in 10 M H<sub>2</sub>SO<sub>4</sub>, the high stability of the passive films was recorded. In the reverse potential scan, no reactivation peak and dissolution of passive films was observed. (vi) In 6 M KOH the passive film on Nb electrode was partially dissolved with apparition of the reactivation peak

whose current intensity is about half intensity of the activation peak. With keeping the electrode at potential of -1.5 V the rest of the film was completely dissolved. (vii) Finally it can conclude that Nb electrode is more resistance in H<sub>2</sub>SO<sub>4</sub> and KOH solutions than the Ti electrode.

## References

- [1] I. Mickova, A. Prusi, T. Grchev, Lj. Arsov, *Portugaliae Electrochimica Acta* **24** (2006) 377-385
- [2] M. A. M. Ibrahim, D. Pongkao, *Journal of Solid State Electrochemistry* **6** (2002) 341-350
- [3] A. Efremova, Lj. Arsov, *Electrochimica Acta* **37** (1992) 2099-2100
- [4] R. Torresi, F. Nart, *Electrochimica Acta* **33** (1988) 1015-1018
- [5] Lj. Arsov, C. Korman, W. Plieth *Journal of Raman Spectroscopy* **22** (1991) 573-575
- [6] J. W. Schultze, M. M. Lohrengel, *Electrochimica Acta* **45** (2002) 2499-2513
- [7] K. Heusler, M. Schultze, *Electrochimica Acta* **20** (1975) 237-244
- [8] A. Prusi, Lj. Arsov, *Corrosion Science* **33** (1992) 153-164
- [9] I. Mickova, *International Review of Chemical Engineering* **2** (2010) 692-701
- [10] W. L. Lee, G. Olive, D. L. Pulfrey L. Young, *Journal of the Electrochemical Society* **117** (1970) 1172-1176
- [11] A. Prusi, Lj. Arsov, B. Haran, B. Popov, *Journal of the Electrochemical Society* **149** (2002) B491-B498
- [12] I. Arsova, Lj. Arsov, N. Hebestreit, A. Anders, W. Plieth, *Journal of Solid State Electrochemistry* **11** (2007) 209-214
- [13] T. Ohtsuka, N. Nomura, *Corrosion Science* **39** (1997) 1253-1263
- [14] I. Mickova, A. Prusi, T. Grchev, Lj. Arsov, *Croatia Chimica Acta* **79** (2006) 527-532
- [15] Lj. Arsov, M. Froelicher, M. Froment, A. Hugot Le-Goff, *Comptes Rendus de l'Académie des Sciences, Paris - Series C – électrochimie* **279** (1974) 485-488
- [16] Lj. Arsov, *Electrochimica Acta* **30** (1995) 1645-1657
- [17] I. A. Amar, S. Darwish, M.W. Khalil, *Materialwissenschaft und Werkstofftechnik*, **12** (1981) 309-315
- [18] S. L. Assis, I. Costa, *Materials Researchs* **10** (2007) 293-296
- [19] M. T. Woldemedhina, D. Raabea, A. W. Hassel, *Electrochimica Acta* **82** (2012) 324-332
- [20] M. K. Han, J. Y. Kim, M. J. Hwang, H. J. Song, Y. J. Park, *Materials* **8** (2015) 5986-6003
- [21] Lj. Arsov, M. Ramasubramanian, B. Popov, *Ellipsometry, Chapter in Book Methods in Materials Research* **1** (2001) 8b.5.1-8b.5.10, John Wiley & Sons Inc.
- [22] A. Efremova, Lj. Arsov, *Journal of Physics France* **2** (1992) 1353-1361